JOURNAL OF BACTERIOLOGY, Jan. 2011, p. 22–29 Vol. 193, No. 1
0021-9193/11/$12.00 doi:10.1128/JB.01143-10

Regulation of Horizontal Gene Transfer in *Bacillus subtilis* by Activation of a Conserved Site-Specific Protease▽

Baundauna Bose and Alan D. Grossman*

Department of Biology, Building 68-530, Massachusetts Institute of Technology, Cambridge, Massachusetts 02139

Received 24 September 2010/Accepted 21 October 2010

The mobile genetic element ICE*Bs1* is an integrative and conjugative element (a conjugative transposon) found in *Bacillus subtilis*. The RecA-dependent SOS response and the RapI-PhrI cell sensory system activate ICE*Bs1* gene expression by stimulating cleavage of ImmR, the ICE*Bs1* immunity repressor, by the protease ImmA. We found that increasing the amount of wild-type ImmA *in vivo* caused partial derepression of ICE*Bs1* gene expression. However, during RapI-mediated derepression of ICE*Bs1* gene expression, ImmA levels did not detectably increase, indicating that RapI likely activates the protease ImmA by increasing its specific activity. We also isolated and characterized mutations in *immA* (*immA*^{h}) that cause partial derepression of ICE*Bs1* gene expression in the absence of inducing signals. We obtained two types of *immA*^{h} mutations: one type caused increased amounts of the mutant proteins *in vivo* but no detectable effect on specific activity *in vitro*; the other type had no detectable effect on the amount of the mutant protein *in vivo* but caused increased specific activity of the protein (as measured *in vitro*). Together, these findings indicate that derepression of ICE*Bs1* gene expression is likely caused by an increase in the specific activity of ImmA. Homologs of ImmA and ImmR are found in many mobile genetic elements, so the mechanisms that regulate ImmA-mediated cleavage of ImmR may be widely conserved.

Integrative and conjugative elements (ICEs), also known as conjugative transposons, are mobile genetic elements found in a wide range of bacteria (reviewed in references 5, 6, 9, 13, 15, and 18). These elements reside in the host chromosome and contribute to genome plasticity. They can facilitate the acquisition of new traits, including antibiotic resistance, symbiosis, and virulence. ICEs can be excised from the host chromosome and transfer to other cells by conjugation. Once inside the recipient, the ICE typically integrates into the host chromosome and is stably maintained and propagated by host replication and cell division. ICEs generally encode proteins that function in regulation, integration, excision, and transfer.

ICE*Bs1* is an approximately 20-kb element inserted in the 3′ end of a tRNA gene in *Bacillus subtilis* (2, 7). Genes at the left end of ICE*Bs1* (Fig. 1A) are part of a regulatory module that resembles those found in many bacteriophages (2, 7). This module includes *immR* and *immA*, encoding the element's immunity repressor and antirepressor, respectively (1, 4). ImmR represses transcription of genes required for excision and transfer and both activates and represses its own expression (1).

ICE*Bs1* gene expression is derepressed *in vivo* during the RecA-dependent SOS response or when the ICE*Bs1*-encoded cell-cell signaling regulator RapI is present and active (Fig. 1B) (2). In both cases, derepression requires the antirepressor ImmA (4). ImmA is a site-specific protease that cleaves ImmR, thereby causing derepression of ICE*Bs1* gene expression (4). It is not known how RapI or RecA stimulate ImmA to cleave ImmR, but previous results indicated that the mechanism of activation was not through transcriptional control of *immA* (4).

We found that increasing the amount or the specific activity of ImmA can cause derepression of ICE*Bs1*, even without activation by RecA or RapI. We isolated and characterized mutations in *immA* that cause derepression of ICE*Bs1* gene expression in the absence of exogenous inducing signals. We also analyzed the effects of artificially elevating the amount of ImmA in the cell. Our results indicate that there are at least two ways in which ImmA-mediated cleavage of ImmR can be activated: (i) by increasing the activity of ImmA or (ii) by increasing the cellular concentration of ImmA. We also found that ImmA levels did not significantly change during activation by RapI, indicating that RapI-mediated induction likely results from an increase in the activity of ImmA.

MATERIALS AND METHODS

Strains and alleles. *B. subtilis* strains used in this study are listed in Table 1. Standard techniques were used for cloning and strain construction (11, 16). The ICE*Bs1*^{0} strain and the *cgeD*::{(P*immR-immR*) *kan*}, *thrC*::{(P*xis-lacZ*Ω343) *mls*}, and the *amyE*::{(P*spank-immA*Ω218) *spc*} alleles were described previously (1, 2, 4). Note that *mls* represents the same gene as the previously used "*erm*" designation. Strains with *recA260* (*cat-mls*) (8) were kept in the dark whenever possible.

P*xyl* and *xylR* from pDR160 (14) were cloned into pMMB752 (3) to generate pBOSE508, a *tet*-containing vector, for introduction of a xylose-inducible gene at *lacA*. A sequence extending from 33 bp upstream of the *rapI* start codon to 2 bp downstream of the stop codon was cloned into pBOSE508 to generate pBOSE525, which was integrated at *lacA* by homologous recombination, selecting for tetracycline resistance.

The sequence from 24 bp upstream of *immA* to 2 bp downstream of its stop codon was cloned downstream from P*spank* into pDR110 (from D. Rudner), a vector that contains *spc*, *lacI*, and P*spank* and that allows for homologous recombination into *amyE*, to generate pBOSE540. Mutations in P*spank-immA* were made by Quikchange (Stratagene) site-directed mutagenesis of pBOSE540. For higher expression of *immA*, P*spank* in pBOSE540 was converted to P*spank*(*hy*) by Quikchange mutagenesis, generating pBOSE1069. The *immA* alleles were intro-

* Corresponding author. Mailing address: Department of Biology, Building 68-530, MIT, Cambridge, MA 02139. Phone: (617) 253-1515. Fax: (617) 253-2643. E-mail: adg@mit.edu.

▽ Published ahead of print on 29 October 2010.

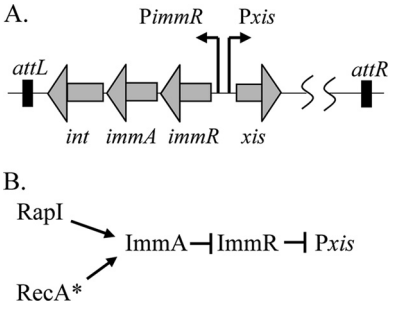

FIG. 1. Regulation of ICE*Bs1*. (A) The four genes and two promoters at the left end of ICE*Bs1* are shown. *immR*, *immA*, and *int* encode the immunity repressor, the antirepressor, and the recombinase (needed for both integration and excision), respectively, and are transcribed leftward from P*immR*. *xis* encodes the excisionase and is transcribed rightward from P*xis*. P*xis* is repressed and P*immR* is both activated and repressed by ImmR (1). Black boxes denote the ends of the element, with the left end in the gene for tRNA-leu2. (B) The circuitry of ICE*Bs1* regulation is shown. ImmR represses transcription from *Pxis*. ImmA inactivates ImmR by proteolytic cleavage, causing derepression of transcription from *Pxis* (4). Cleavage of ImmR by ImmA occurs *in vivo* during the RecA-dependent SOS response (RecA*) or when the ICE*Bs1*-encoded cell-cell signaling regulator RapI is present and active (2).

duced into wild-type cells by a double crossover at *amyE*, selecting for spectinomycin resistance.

Escherichia coli strains derived from BL21-AI (Invitrogen) were used to purify ImmR and ImmA. N-terminally His-tagged ImmR was purified from BOSE798, and untagged ImmA was purified from BOSE848 (4). *immA* mutations were introduced by Quikchange mutagenesis of pBOSE831 (4), and the resulting plasmids were introduced into *E. coli* BL21-AI to produce BOSE843 (R85G), BOSE844 (V92E), BOSE845 (N93D), BOSE846 (I165*), BOSE1133 (I160*), and BOSE1134 (G169*).

Media and growth conditions. *B. subtilis* cells were grown at 37°C with aeration in defined S7 minimal salts medium (17), except that MOPS (morpholinepropanesulfonic acid) buffer was used at 50 mM instead of 100 mM. The medium also contained 1% arabinose, 0.1% glutamate, 40 μg/ml tryptophan and phenylalanine, and 120 μg/ml threonine. Xylose (1%) was used to induce expression of P*xyl-rapI*. When appropriate, antibiotics (at the indicated concentrations) were used as follows: chloramphenicol (5 μg/ml), kanamycin (5 μg/ml), tetracycline (10 μg/ml), and spectinomycin (100 μg/ml); erythromycin (0.5 μg/ml) and lincomycin (12.5 μg/ml) were used together to select for macrolide-lincosamide-streptogramin B (MLS) resistance. Mitomycin-C (Roche) was used at a final concentration of 1 μg/ml. X-Gal (5-bromo-4-chloro-3-indolyl α-D-galactopyranoside) in LB agar plates was used at 120 μg/ml.

E. coli cells used to overproduce ImmA and ImmR were grown in LB medium at 30°C or 37°C. When appropriate, ampicillin (100 to 200 μg/ml) and/or chloramphenicol (15 μg/ml) was added. To induce gene expression in BL21-AI cells (Invitrogen), the growth medium was supplemented with ≥1 mM IPTG (isopropyl-β-D-thiogalactopyranoside) and 0.2% arabinose.

ImmA^h mutant hunt. Identification of hyperactive *immA* mutants was based on screening the expression of a P*xis-lacZ* fusion. In the presence of the ImmR repressor, cells containing P*xis-lacZ* are white on X-Gal indicator plates because P*xis-lacZ* is efficiently repressed. Cells with wild-type *immA* or a nonfunctional *immA* are also white. A hyperactive ImmA protein should cleave and inactivate ImmR, causing derepression of P*xis-lacZ* and leading to visualization of blue colonies on X-Gal.

immA was amplified from chromosomal DNA (strain JH642) by mutagenic PCR in the presence of $MnCl_2$ by the use of *Taq* DNA polymerase (1.25 units in a 50-μl reaction mixture) under conditions recommended by the supplier (Roche). Products were cloned downstream of the LacI-repressible, IPTG-inducible promoter P*spank* in pDR110 vector. Ligation mixtures were used to transform competent *E. coli* DH5α cells, selecting for ampicillin resistance. Transformants from a single PCR were pooled, and plasmid DNA was prepared from each pool and used to transform the *B. subtilis* BOSE533 strain (containing P*xis-lacZ* and *immR*). Transformants were grown on LB plates containing spectinomycin (to select transformants), IPTG (to induce P*spank-immA*), and X-Gal (to visualize P*xis-lacZ* expression). Blue colonies were picked and restreaked to purify single colonies. Each candidate colony was grown in liquid LB, and genomic DNA was purified from these cells. This DNA was used to transform the BOSE533 indicator strain, selecting for the *spc* marker associated with P*spank-immA* at *amyE* and screening for blue coloration (in the presence of IPTG when used to express P*spank-immA*). Genomic DNA from a candidate that produced blue transformants indicated that the blue phenotype was caused by a mutation linked to *spc* at *amyE*, most likely a mutation that made ImmA hyperactive. To verify this, *immA* was amplified from this DNA by high-fidelity PCR (Platinum *Taq* DNA polymerase; Invitrogen), and the PCR products were sequenced (MIT Biopolymers Laboratory).

Mutations identified in the candidates were reconstructed by site-directed mutagenesis of *immA* in pBOSE540 (pDR110-*immA*) (by use of Quikchange site-directed mutagenesis; Stratagene), and the resulting plasmids were introduced into JH642 by double crossovers at *amyE*. Genomic DNA from these strains was used to introduce each *immA^h* allele into indicator strains such as BOSE533.

Western blot analysis. Samples collected from *B. subtilis* cultures were flash-frozen (liquid nitrogen) and stored at −20°C before being thawed and pelleted, or they were pelleted immediately. Cell pellets were washed with TN buffer (50 mM Tris, 300 mM NaCl, pH 8) and stored at −20°C. Cell pellets were thawed and resuspended in buffer (10 mM Tris, 10 mM EDTA, pH 7) containing 0.1 mg/ml lysozyme and the protease inhibitor 4-(2-aminoethyl) benzenesulfonyl fluoride hydrochloride (AEBSF) at 1 mM. The volume of buffer used to resuspend each sample of cells was adjusted to the optical density at 600 nm (OD_{600}) in order to normalize the concentration of proteins in each sample. Resuspended cells were incubated at 37°C for 30 min, SDS sample buffer was added, and samples were heated at 100°C for 10 min followed by centrifugation to remove insoluble material.

Proteins were separated by sodium dodecyl sulfate-polyacrylamide gel elec-

TABLE 1. *B. subtilis* strains[a]

Strain	Genotype description
BOSE533	ICE*Bs1*^{0} *thrC*::{(P*xis-lacZ*Ω343) *mls*} *cgeD*::{(P*immR-immR*) *kan*} *lacA*::{(P*xyl-rapI*) *tet*}
BOSE534	ICE*Bs1*^{0} *thrC*::{(P*xis-lacZ*Ω343) *mls*} *cgeD*::{(P*immR-immR*) *kan*} *amyE*::{(P*spank-immA*Ω218) *spc*} *lacA*::{(P*xyl-rapI*) *tet*}
BOSE569	ICE*Bs1*^{0} *thrC*::{(P*xis-lacZ*Ω343) *mls*} *cgeD*::{(P*immR-immR*) *kan*} *amyE*::{(P*spank-immA*(*R85G*)Ω218) *spc*} *lacA*::{(P*xyl-rapI*) *tet*}
BOSE672	ICE*Bs1*^{0} *thrC*::{(P*xis-lacZ*Ω343) *mls*} *cgeD*::{(P*immR-immR*) *kan*} *amyE*::{(P*spank-immA*(*N93D*)Ω218) *spc*} *lacA*::{(P*xyl-rapI*) *tet*}
BOSE708	ICE*Bs1*^{0} *thrC*::{(P*xis-lacZ*Ω343) *mls*} *cgeD*::{(P*immR-immR*) *kan*} *amyE*::{(P*spank-immA*(*V92E*)Ω218) *spc*} *lacA*::{(P*xyl-rapI*) *tet*}
BOSE713	ICE*Bs1*^{0} *thrC*::{(P*xis-lacZ*Ω343) *mls*} *cgeD*::{(P*immR-immR*) *kan*} *amyE*::{(P*spank-immA*(*I165**)Ω218) *spc*} *lacA*::{(P*xyl-rapI*) *tet*}
BOSE904	ICE*Bs1*^{0} *thrC*::{(P*xis-lacZ*Ω343) *mls*} *cgeD*::{(P*immR-immR*) *kan*} *amyE*::{(P*spank-immA*(*G169**)Ω218) *spc*} *lacA*::{(P*xyl-rapI*) *tet*}
BOSE912	ICE*Bs1*^{0} *thrC*::{(P*xis-lacZ*Ω343) *mls*} *cgeD*::{(P*immR-immR*) *kan*} *amyE*::{(P*spank-immA*(*I160**)Ω218) *spc*} *lacA*::{(P*xyl-rapI*) *tet*}
BOSE1071	ICE*Bs1*^{0} *thrC*::{(P*xis-lacZ*Ω343) *mls*} *cgeD*::{(P*immR-immR*) *kan*} *amyE*::{(P*spank-immA*(*R85G*)Ω218) *spc*} *recA260*::*cat-mls*
BOSE1073	ICE*Bs1*^{0} *thrC*::{(P*xis-lacZ*Ω343) *mls*} *cgeD*::{(P*immR-immR*) *kan*} *amyE*::{(P*spank-immA*(*V92E*)Ω218) *spc*} *recA260*::*cat-mls*
BOSE1074	ICE*Bs1*^{0} *thrC*::{(P*xis-lacZ*Ω343) *mls*} *cgeD*::{(P*immR-immR*) *kan*} *amyE*::{(P*spank-immA*(*I165**)Ω218) *spc*} *recA260*::*cat-mls*
BOSE1076	ICE*Bs1*^{0} *thrC*::{(P*xis-lacZ*Ω343) *mls*} *cgeD*::{(P*immR-immR*) *kan*} *amyE*::{(P*spank-immA*(*G169**)Ω218) *spc*} *recA260*::*cat-mls*
BOSE1095	ICE*Bs1*^{0} *thrC*::{(P*xis-lacZ*Ω343) *mls*} *cgeD*::{(P*immR-immR*) *kan*} *amyE*::{(P*spank*(*hy*)*-immA*Ω218) *spc*} *lacA*::{(P*xyl-rapI*) *tet*}
BOSE1110	ICE*Bs1*^{0} *thrC*::{(P*xis-lacZ*Ω343) *mls*} *cgeD*::{(P*immR-immR*) *kan*} *amyE*::{(P*spank-immA*(*R85G*, *I165**)Ω218) *spc*} *lacA*::{(P*xyl-rapI*) *tet*}
BOSE1111	ICE*Bs1*^{0} *thrC*::{(P*xis-lacZ*Ω343) *mls*} *cgeD*::{(P*immR-immR*) *kan*} *amyE*::{(P*spank-immA*(*V92E*, *I165**)Ω218) *spc*} *lacA*::{(P*xyl-rapI*) *tet*}
BOSE1237	ICE*Bs1*^{0} *thrC*::{(P*xis-lacZ*Ω343) *mls*} *cgeD*::{(P*immR-immR*) *kan*} *amyE*::{(P*spank-immA*(*V92E*, *G169**)Ω218) *spc*} *lacA*::{(P*xyl-rapI*) *tet*}
BOSE1257	ICE*Bs1*^{0} *thrC*::{(P*xis-lacZ*Ω343) *mls*} *cgeD*::{(P*immR-immR*) *kan*} *amyE*::{(P*spank-immA*(*V92E*, *N93D*)Ω218) *spc*} *lacA*::{(P*xyl-rapI*) *tet*}

[a] All strains were derived from laboratory strain JH642 and contained *trpC* and *pheA* mutations.

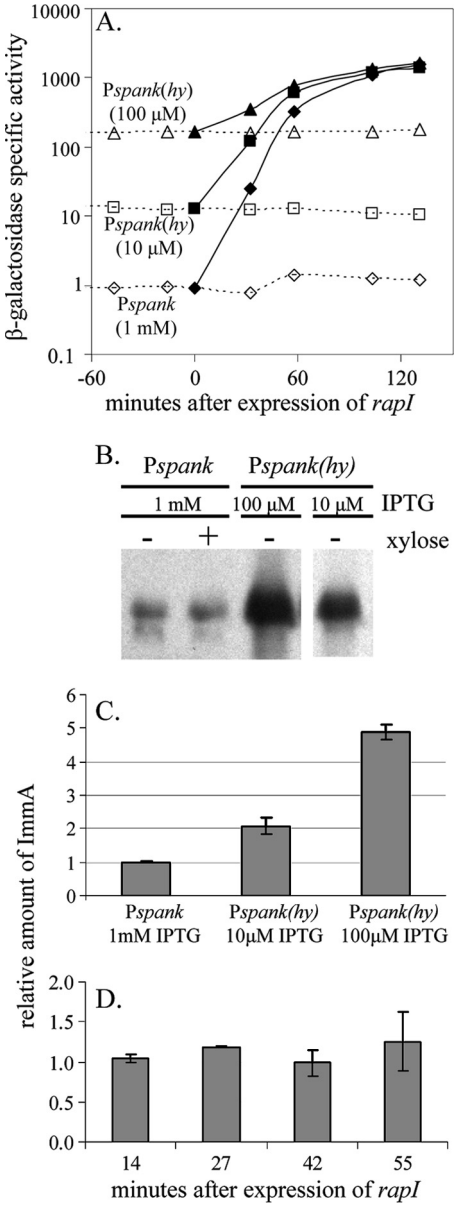

FIG. 2. Effects of ImmA levels on expression of P*xis-lacZ*. All strains were cured of ICE*Bs1* (ICE*Bs1*^{0}) and expressed *immR*, *immA*, and *rapI* at ectopic loci. Expression of *immA* from P*spank* or the stronger P*spank*(*hy*) was controlled with different concentrations of IPTG. Cells were grown in defined minimal medium with arabinose at 37°C. At $t = 0$, cultures were split and xylose was added to one part to induce expression of P*xyl-rapI*. Effects on ICE*Bs1* gene expression were monitored using a P*xis-lacZ* fusion, and levels of ImmA protein were determined by Western blotting with anti-ImmA antibodies. (A) ß-Galactosidase activity is plotted as a function of time relative to the addition of xylose to induce expression of P*xyl-rapI*. Open symbols, untreated; closed symbols, treated with xylose at time 0; diamonds, P*spank-immA* (BOSE534) with 1 mM IPTG; squares, P*spank*(*hy*) (BOSE1095) with 10 μM IPTG; triangles, P*spank-immA* (BOSE1095) with 100 μM IPTG. (B) The relative amounts of ImmA were compared on Western blots with anti-ImmA antibodies. Equivalent amounts of cell extracts from the indicated samples, with IPTG to induce expression of *immA* and with or without xylose to induce expression of *rapI*, were loaded in each lane. Strains were the same as described for panel A. (C) The amount of ImmA relative to that in cells with P*spank-immA* (BOSE534) grown with 1 mM IPTG is plotted. Results from cells with P*spank*(*hy*)-*immA* (BOSE1095) grown with 10 μM and 100 μM IPTG are also shown. For each time point, the average value for two replicates is plotted, and the error bar indicates 1 standard deviation above and below the average. (D) The ratio of ImmA in xylose-treated samples to that in untreated samples is plotted for cells with P*spank-immA* (BOSE534) grown with 1 mM IPTG. The time at which samples were taken is indicated below each bar as minutes after splitting of the culture for treatment with xylose. For each time point, the average value for at least two replicates is plotted, and the error bar indicates 1 standard deviation above and below the average.

trophoresis (SDS-PAGE) on 15% or 18% gels and transferred to a PolyScreen polyvinylidene difluoride (PVDF) membrane (Perkin Elmer) using a Trans-blot semidry electroblot transfer apparatus (Bio-Rad). Membranes were blocked in 0.2% I-Block (Tropix)–TBST (50 mM Tris, 200 mM NaCl, 0.05% Tween 20, pH 8) either at room temperature for 1 h or overnight at 4°C. The PVDF membranes were incubated in a 1:5,000 dilution of anti-ImmA rabbit polyclonal antisera (made commercially by Covance using ImmA-His6 protein purified from *E. coli*) in 0.2% I–Block TBST for 1 h at room temperature, washed several times in TBST, incubated in 1:3,000 goat anti-rabbit IgG-horseradish peroxidase (IgG-HRP) conjugate (Bio-Rad) for 1 h at room temperature, and washed several times in TBST. Signals were detected using Western Lightning chemiluminescence reagents (Perkin-Elmer) followed by exposure to Kodak Biomax light film.

The amount of ImmA in *B. subtilis* lysates was quantified by comparison to purified ImmA on Western blots with anti-ImmA antibodies. Films were scanned and densities were assessed using ImageQuant TL (GE Healthcare). For each blot, a standard curve was generated using at least four different quantities of purified ImmA. ImmA levels that fell within the linear range of the standard curve for each blot were measured for each *B. subtilis* sample. For each *B. subtilis* sample, two or more independent measurements of ImmA level by Western blotting were averaged.

β-Galactosidase assays. β-Galactosidase specific activity was assayed as described previously (12). Specific activity was calculated relative to the optical density at 600 nm of the samples. Results shown are from a single experiment and are representative of results obtained in at least three independent experiments, except for Fig. 2A, which shows the results of one experiment.

Protein purification and *in vitro* assays. N-terminally His-tagged ImmR, untagged ImmA, and untagged mutants of ImmA were purified and assayed as previously described (4).

RESULTS

Overexpression of *immA* can derepress P*xis-lacZ*. Previous experiments indicated that cells with C-terminally epitope-tagged ImmA had elevated ImmA protein levels and a small increase in ICE*Bs1* gene expression (J. M. Auchtung and A. D. Grossman, unpublished results). Based on these results, we decided to directly test the relationship between levels of native (untagged) ImmA and transcription from the major promoter in ICE*Bs1*. We used transcription of a P*xis-lacZ* fusion as an indicator of ICE*Bs1* gene expression. P*xis* is strongly repressed by ImmR (1). Derepression requires ImmA and occurs after overexpression of *rapI* or during the RecA-mediated SOS response (4). This regulation occurs in both the presence and the absence of all other ICE*Bs1* genes (1, 4). For simplicity, the experiments presented here were done with cells lacking ICE*Bs1* (ICE*Bs1*^{0}).

We found that increased expression of *immA* caused increased expression of P*xis-lacZ*. We modulated expression of *immA* by the use of a fusion to the IPTG-inducible promoter P*spank* (P*spank-immA*) or to the stronger P*spank*(*hy*) [P*spank*(*hy*)-*immA*] promoter and by adjusting *immA* expression levels with different concentrations of IPTG. The cells contained *immR*, expressed from its own promoter, and a copy

of *rapI* fused to the xylose-inducible promoter P*xyl* (P*xyl-rapI*) but were grown in the absence of xylose. Expression of P*xis-lacZ* (Fig. 2A) was low (~1 specific activity unit) when cells containing the weaker P*spank-immA* fusion were grown with 1 mM IPTG (fully induced P*spank*). Expression of P*xis-lacZ* was higher (~10 specific activity units) when cells containing P*spank*(*hy*)-*immA* were grown with 10 μM IPTG and higher still (~150 specific activity units) when grown with 100 μM IPTG (Fig. 2A). Expression of P*xis-lacZ* was fully derepressed (~1,000 specific activity units) when cells containing P*spank*(*hy*)-*immA* were grown with 1 mM IPTG (data not shown) or when *rapI* was overexpressed from P*xyl-rapI* following the addition of xylose (see below).

We measured relative levels of ImmA protein (in Western blots with anti-ImmA antibodies) under the conditions used for monitoring expression of P*xis-lacZ*. As expected, the relative amounts of ImmA increased with higher concentrations of IPTG (Fig. 2B and C). In cells with a >5-fold increase in the amount of ImmA [from P*spank*(*hy*)-*immA* with 100 μM IPTG compared to the fully induced weaker P*spank-immA*], there was an approximately 150-fold increase in ß-galactosidase specific activity (Fig. 2A). These results indicate that increased levels of ImmA cause increased transcription from P*xis*.

Induction of P*xis-lacZ* by overexpression of RapI does not cause an increase in the amount of ImmA. Although increasing the amount of ImmA caused increased expression of P*xis-lacZ*, the amount of ImmA did not increase when expression of P*xis-lacZ* was induced by overproduction of RapI. Addition of xylose to induce expression of *rapI* (from P*xyl-rapI*), in cells with P*spank-immA* grown with 1 mM IPTG, caused an increase in expression of P*xis-lacZ* (Fig. 2A). By approximately 60 min after expression of RapI, there was a >100-fold increase in ß-galactosidase specific activity, and after 90 to 120 min, there was an approximately 1,000-fold increase in ß-galactosidase specific activity (Fig. 2A). Under these conditions, there was little or no detectable change in the amount of ImmA (Fig. 2B and D). These results indicate that P*xis-lacZ* is derepressed by RapI even though *immA* is expressed from a heterologous promoter and that derepression can occur without a significant increase in the amount of ImmA. Importantly, the increase in transcription from P*xis* with no detectable change in ImmA levels was significantly greater than that caused by an approximately 5-fold increase in ImmA.

Isolation of hyperactive mutants of ImmA. To better understand the mechanisms of derepression of ICE*Bs1* gene expression, we isolated and characterized mutations in *immA* (*immA*^{h}) that cause increased expression of P*xis-lacZ* without exogenous induction, i.e., without induction of the SOS response and without overexpression of *rapI*. In the presence of the repressor ImmR, cells containing P*xis-lacZ* are white on X-Gal indicator plates because P*xis-lacZ* is efficiently repressed. Cells with wild-type *immA* or a nonfunctional *immA* are also white. A hyperactive ImmA should cleave and inactivate ImmR, causing derepression of P*xis-lacZ* and leading to the visualization of blue colonies on X-Gal.

We used a strain (BOSE533) that contains P*xis-lacZ*, expresses *immR* from its own promoter (to repress P*xis-lacZ*), and has a P*xyl-rapI* fusion. We introduced mutagenized *immA* under the control of P*spank* into these cells and screened for mutants that formed blue colonies (in the presence of IPTG),

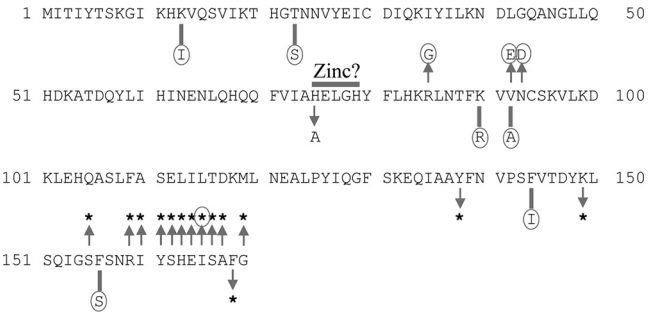

FIG. 3. ImmA sequence and mutations. The complete amino acid sequence of ImmA is shown. The horizontal bar indicates the putative zinc-binding motif HELGH. Single amino acid substitutions are shown above and below the sequence. Circled mutations were identified in the mutant hunt, remade, and tested. Arrows pointing up indicate mutations that cause a hyperactive phenotype. Arrows pointing down indicate mutations that cause a null phenotype. Vertical bars indicate mutations that maintain the wild-type phenotype. Stars indicate stop codons.

indicating at least partial derepression of P*xis-lacZ*. The *immA* alleles from candidate mutants were backcrossed and cells retested to be sure the mutant phenotype was linked to *immA*. Mutant *immA* alleles were then sequenced. Since several alleles contained multiple mutations, we reconstructed each single mutation by site-directed mutagenesis of *immA* and tested each for effects on expression of P*xis-lacZ* (Materials and Methods). Each mutation is designated by the amino acid in wild-type ImmA, its position in the sequence, and the amino acid to which it was changed. Changes to a stop codon are designated with an asterisk (*). Single mutations causing K13I, T23S, R85G, K90R, V92A, V92E, N93D, F144I, F156S, and I165* were remade (Fig. 3). Four of these caused significantly increased expression of P*xis-lacZ* (see below), and the others had little or no effect on expression of P*xis-lacZ* (data not shown) and were not characterized further.

Four mutations in *immA* (R85G, V92E, N93D, and I165*) caused increased expression of P*xis-lacZ* on X-Gal indicator plates, indicating that they somehow caused ImmA to be hyperactive. Three of these mutations (R85G, V92E, and N93D) are in the central region of ImmA, just C terminal to the predicted zinc-binding motif HEXXH (Fig. 3). The I165* mutation truncates the protein by five amino acids at its C terminus. We further explored the effect of truncating ImmA at its C terminus by targeted mutagenesis. Nonsense mutations at positions 155, 159 through 167, and 169 caused a hyperactive phenotype, and nonsense mutations at positions 138, 149, and 168 caused a null phenotype (Fig. 3), as detected on X-Gal indicator plates.

Effects of ImmA^h mutants on expression of P*xis-lacZ*. We further characterized the three central missense mutations (R85G, V92E, and N93D) and three of the C-terminal nonsense mutations (I160*, I165*, and G169*). All three caused an increase in expression of P*xis-lacZ* in cells grown in defined liquid medium (Fig. 4), although to different extents. R85G had the largest effect (Fig. 4A and C) and G169* the smallest (Fig. 4B and D). Expression of P*xis-lacZ* in the R85G mutant appeared to be fully derepressed, and expression in all the other mutants was further increased after overexpression of

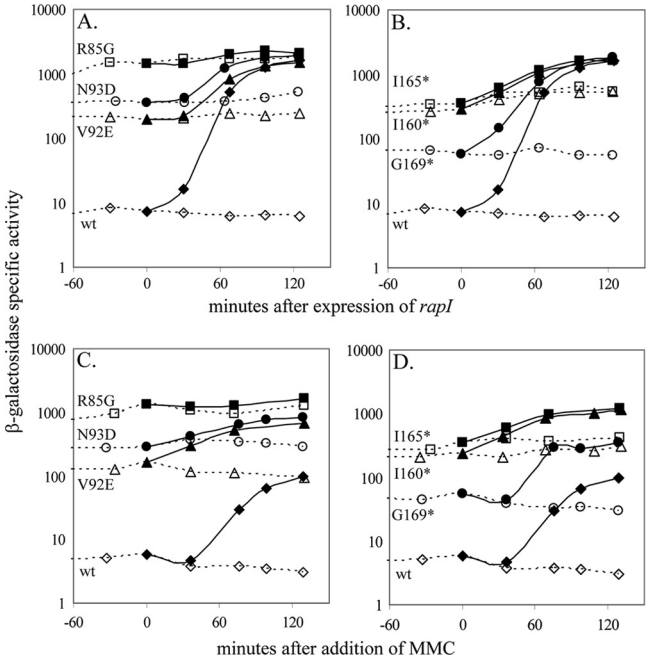

FIG. 4. Effects of ImmA^h mutants on P*xis-lacZ*. All strains were cured of ICE*Bs1* (ICE*Bs1*^{0}) and expressed *immR*, *immA*, and *rapI* at ectopic loci. Strains harboring *immA*^{h} mutants were compared to the wild type. Cultures were grown in defined minimal medium with 1 mM IPTG for continuous expression of *immA* variants from P*spank*. At t = 0, cultures were split, and one part was treated with xylose to induce expression of P*xyl-rapI* (panels A and B, closed symbols) or with MMC to induce the SOS response (panels C and D, closed symbols).The other part of each culture was left untreated (open symbols). Effects on ICE*Bs1* gene expression were monitored using a P*xis-lacZ* fusion. (A and C) *immA*^{h} variants with mutations near the center of ImmA's sequence. Wild type (BOSE534), diamonds; R85G (BOSE569), squares; V92E (BOSE708), triangles; N93D (BOSE672), circles. (B and D) *immA*^{h} variants with mutations near ImmA's C terminus. Wild type (BOSE534), diamonds; I160* (BOSE912), triangles; I165* (BOSE713), squares; G169* (BOSE904), circles.

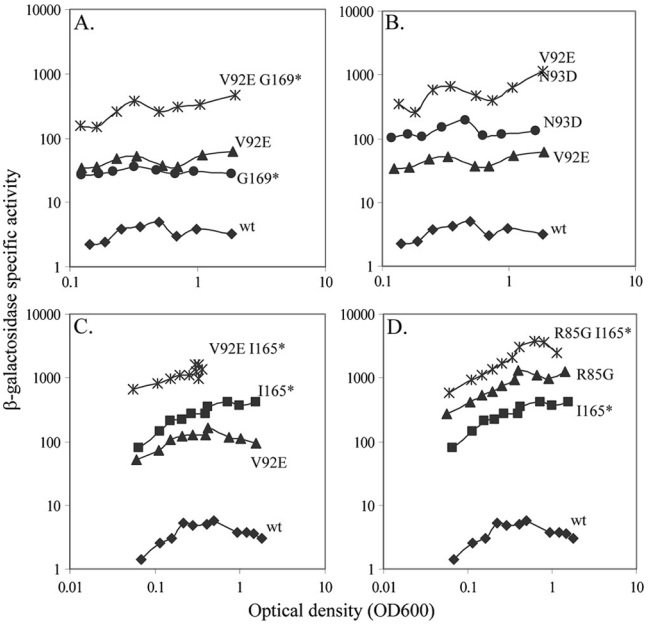

FIG. 5. Effects on P*xis-lacZ* expression of *immA* alleles that contain two mutations, either of which causes a hyperactive phenotype. All strains were cured of ICE*Bs1* (ICE*Bs1*^{0}) and expressed *immR* and *immA* at ectopic loci. Cultures were grown in defined minimal medium with 1 mM IPTG for expression of *immA* from P*spank*. Effects on ICE*Bs1* gene expression were monitored using a P*xis-lacZ* fusion. ß-Galactosidase activity is plotted as a function of the OD_{600} of the culture. In all panels, BOSE534, the wild-type (wt) strain, is indicated with diamonds. ImmA mutants are indicated by the identity and position of the amino acid change. (A) V92E (BOSE708), triangles; G169* (BOSE904), circles; V92E G169* (BOSE1237), asterisks. (B) V92E (BOSE708), triangles; N93D (BOSE672), circles; V92E N93D (BOSE1257), asterisks. Data for the wild type and V92E are the same as described for panel A. (C) V92E (BOSE708), triangles; I165* (BOSE713), squares; V92E I165* (BOSE1111), asterisks. (D) R85G (BOSE569), triangles; I165* (BOSE713), squares; R85G I165* (BOSE1110), asterisks. Data for the wild type and I165* are the same as described for panel C.

rapI, with all strains reaching the same maximum level of P*xis-lacZ* expression (Fig. 4A and B).

Expression of P*xis-lacZ* in the mutants was also further increased after the addition of mitomycin C (MMC) to induce a DNA damage response. In these experiments, strains with higher uninduced (no MMC) levels of P*xis-lacZ* expression had a higher induced level of ß-galactosidase specific activity than those with lower uninduced expression levels (Fig. 4C and D). This is consistent with the typically lower induction of ICE*Bs1* seen in response to MMC than in response to RapI (2). In addition, the presence of MMC caused a decrease in cell growth and viability as judged by a drop in the OD_{600} ~2 h after treatment, indicating that cells may have begun to die before all the strains could accumulate the maximum level of ß-galactosidase.

We constructed several alleles of *immA* that contained two mutations, each of which causes a hyperactive phenotype. The double mutants V92E G169* (Fig. 5A), V92E I165* (Fig. 5B), V92E N93D (Fig. 5C), and R85G I165* (Fig. 5D) all caused higher expression of P*xis-lacZ* than either of the respective single mutations (Fig. 5). A fifth combination, N93D S155*, showed higher expression of P*xis-lacZ* than one of the single mutants (S155*) but less than the other (N93D) (data not shown). These results indicate that, for some of the combinations, the effects on expression of P*xis-lacZ* appear to be additive, which is consistent with the notion that the central and C-terminal mutants might have different effects on ImmA.

RapI and RecA are not required for ImmA^h phenotypes. The ImmA^h mutants respond to both RapI and DNA damage, and the strain background in which we isolated the *immA*^{h} mutants was *recA*$^+$ and contained P*xyl-rapI*. Therefore, we tested whether the ImmA^h mutants required endogenous RecA and perhaps low-level (leaky) expression of P*xyl-rapI* under otherwise noninducing conditions. We found that the *immA*^{h} mutations tested (R85G, V92E, I165*, and G169*) all caused elevated expression of P*xis-lacZ* in a *recA* null mutant in the absence of *rapI* (Fig. 6A), although expression was about 20% of that seen in *recA*$^+$ cells with P*xyl-rapI* (Fig. 6B). In cells producing wild-type ImmA, expression of P*xis-lacZ* was similarly reduced in the *recA* mutant in the absence of *rapI* (Fig. 6), indicating that much of this effect was independent of the *immA*^{h} mutations. These findings indicate that the ImmA^h

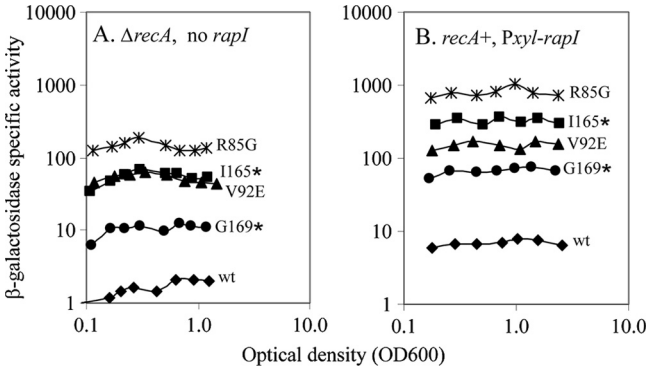

FIG. 6. Effects of *rapI* and *recA* on P*xis-lacZ* expression. All strains were cured of ICE*Bs1* (ICE*Bs1*^{0}) and expressed *immR* and *immA* at ectopic loci. Cells harbored wild-type *immA* or an *immA*^{h} mutant. Cultures were grown in defined minimal medium with 1% arabinose and 1 mM IPTG for expression of *immA* from P*spank*. Effects on ICE*Bs1* gene expression were monitored using a P*xis-lacZ* fusion. ß-Galactosidase activity is plotted as a function of the OD_{600} of the culture. (A) Strains lack the P*xyl-rapI* construct, harbor a null mutation of *recA*, and express the indicated allele of *immA*. Wild type (BOSE1256), diamonds; R85G (BOSE1071), asterisks; V92E (BOSE1073), triangles; I165* (BOSE1074), squares; G169* (BOSE1076), circles. (B) Strains that had the ectopic P*xyl-rapI* construct and wild-type *recA* and expressed the indicated allele of *immA*. Expression from P*xyl* was not induced. Wild type (BOSE534), diamonds; R85G (BOSE569), asterisks; V92E (BOSE708), triangles; I165* (BOSE713), squares; G169* (BOSE904), circles.

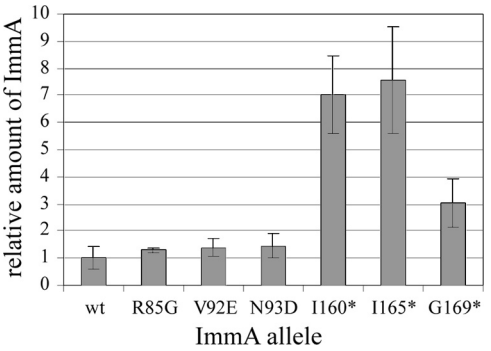

FIG. 7. Cellular levels of ImmA^h mutant proteins. Levels of ImmA protein in strains expressing different alleles of *immA* were determined by Western blotting with anti-ImmA antibodies. For each strain, ImmA levels were quantified, and the averages of the results for at least three samples were calculated. The average for each type of ImmA was then normalized to the average for wild-type ImmA and plotted. Error bars indicate 1 standard deviation above and below each mean. Samples were taken from cells grown in defined minimal medium with 1 mM IPTG for expression of *immA* from P*spank*. All strains expressed *immR* from its own promoter. Data represent the wild type (wt) (BOSE534), the three central mutants, R85G (BOSE569), V92E (BOSE708), and N93D (BOSE672), and three C-terminal mutants, I160* (BOSE912), I165* (BOSE713), and G169* (BOSE904).

mutants are hyperactive in the absence of either of the known inducers (RecA and RapI).

ImmA C-terminal truncation mutants have increased protein levels *in vivo*. Because elevated levels of ImmA caused increased expression of P*xis-lacZ* (Fig. 2), we determined whether any of the *immA*^{h} mutations caused an increase in the amount of ImmA in the cell. We measured relative amounts of wild-type ImmA and six ImmA^h mutants by the use of Western blots with anti-ImmA antibodies. Each of the three central ImmA^h mutants (R85G, V92E, and N93D) was present in the cell at a level similar to that seen with wild-type ImmA (Fig. 7). In contrast, the three C-terminal mutants examined (I160*, I165*, and G169*) had significantly higher protein levels *in vivo* compared to wild-type ImmA levels (Fig. 7). There was approximately 3-fold more ImmAG169* and approximately 7-fold more ImmAI160* and ImmAI165* than wild-type ImmA. These relative levels are consistent with the effect of each of the truncation mutations on expression of P*xis-lacZ* (Fig. 4). It seems most likely that the truncation mutations affect stability of ImmA, indicating that the wild-type protein is normally unstable. Initial results from screening known cellular protease mutants indicated that ImmA levels were significantly higher in a *clpP* mutant (B. Bose and A. D. Grossman, unpublished results). We conclude that the truncation mutations likely cause increased expression of P*xis-lacZ* due to increased stability of the mutant ImmA protein and that the central mutations likely cause increased expression of P*xis-lacZ* by some other mechanism.

Central *immA*^{h} mutations increase the activity of ImmA *in vitro*. The ability of the central ImmA^h mutant proteins to cleave ImmR *in vitro* was greater than that of wild-type ImmA or the truncation mutants. We purified the three central mutants (R85G, V92E, and N93D) and three C-terminal truncations (I160*, I165*, and G169*) and compared the abilities of these ImmA mutants to cleave ImmR (His6-ImmR) *in vitro*. The C-terminal truncations all cleaved ImmR (His6-ImmR) at a rate comparable to that of wild-type ImmA (Fig. 8). In these reactions, less than 50% of the ImmR was cleaved by wild-type ImmA after 180 min, as judged by the appearance of a fragment of ImmR and the ratio of the amount of the fragment to that of full-length ImmR (Fig. 8).

In contrast, all three central ImmA mutants cleaved ImmR significantly faster than did wild-type ImmA (Fig. 8). In these reactions, >90% of the ImmR was cleaved by each ImmA mutant within 180 min (Fig. 8). The R85G mutant appeared to be the most active, which is consistent with the *in vivo* effects on expression of the presence of P*xis-lacZ* (Fig. 4). Together, our results indicate that the C-terminal truncation mutations affect the amount of ImmA protein *in vivo* but do not have a significant effect on ImmA specific activity and that the central mutations primarily affect the specific activity of ImmA and do not significantly affect ImmA levels *in vivo*.

DISCUSSION

Our results indicate that there are at least two ways to increase ImmA-mediated proteolysis of ImmR to cause derepression of ICE*Bs1* gene expression: (i) by increasing the amount of ImmA and (ii) by increasing the specific activity of ImmA. We found that RapI (and probably RecA) likely activates ICE*Bs1* by causing an increase in the specific activity of ImmA *in vivo*.

ImmA levels and derepression of P*xis*. We found that increasing the amount of wild-type ImmA, by increasing its production from a heterologous promoter, caused increased expression of P*xis-lacZ*, a reporter for ICE*Bs1* gene expression.

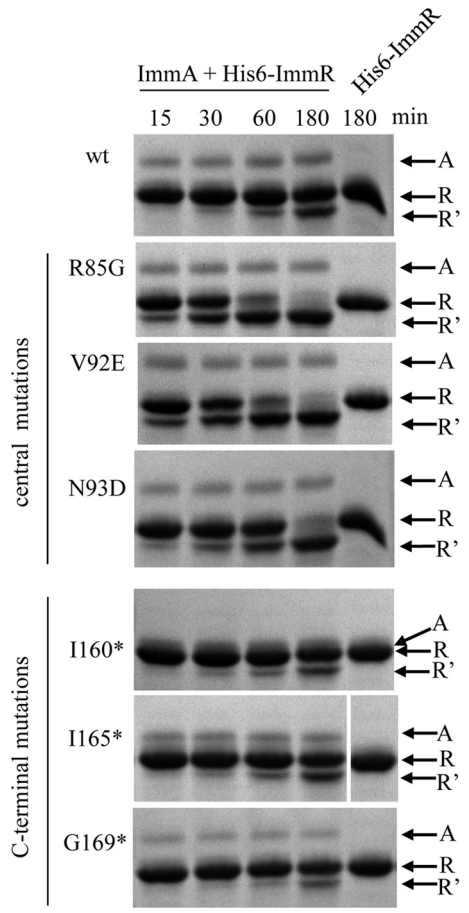

FIG. 8. *In vitro* proteolysis of ImmR by ImmA^h mutants. His6-ImmR (180 μM) and ImmA (12 μM) were incubated together at 37°C for the times indicated above each column. Reaction products were visualized by Coomassie-stained SDS-PAGE. Each row shows results obtained using reaction mixtures containing a single ImmA variant (or no ImmA, for the last column) at successive time points. Wild-type ImmA and six ImmA^h mutants were tested. ImmA (A), intact His6-ImmR (R), or the N-terminal fragment of His6-ImmR (R') is marked to the right of each row. ImmAI160* migrates to a position barely distinguishable from that of intact His6-ImmR, so the ImmR fragment can be used to gauge the progress of these reactions.

Preliminary measurements indicate that ImmA levels are significantly increased in a *clpP* protease mutant (Bose and Grossman, unpublished). In addition, truncations of ImmA that removed several C-terminal amino acids also caused an increase in the amount of ImmA and an increase in expression of P*xis-lacZ*. These findings indicate that ImmA is normally unstable and that this instability is influenced by C-terminal residues of ImmA. There are many examples of regulatory proteins that are constitutively degraded, allowing for rapid changes in their intracellular concentrations when they are stabilized against proteolysis (10).

Although increasing the amount of ImmA in the cell caused derepression of ICE*Bs1* gene expression, this does not seem to be the primary mechanism for derepression in response to RapI. The amount of ImmA did not detectably change when P*xis-lacZ* expression was induced by production of RapI. Under these conditions, there was an approximately 1,000-fold increase in ß-galactosidase specific activity from P*xis-lacZ*. When the amount of wild-type ImmA was increased approximately 4- to 5-fold, there was an approximately 100-fold increase in ß-galactosidase specific activity from P*xis-lacZ*, significantly less than the increase in expression caused by RapI. These findings indicate that something other than an increase in ImmA levels causes RapI-dependent derepression of ICE*Bs1* gene expression.

Mutations that increase the specific activity of ImmA. We also isolated mutations that affect the central part of ImmA, near the putative metal-binding motif, and that cause an increase in ICE*Bs1* gene expression. In contrast to the C-terminal truncation mutations that affect the levels of ImmA, these mutations do not detectably affect the cellular concentration of ImmA. Rather, these ImmA mutant proteins were more efficient than the wild type at cleaving ImmR both *in vivo* and *in vitro*, and these effects were generally consistent with the effects on P*xis-lacZ* expression *in vivo*. These findings indicate that the mutations cause an increase in the specific activity of ImmA.

There are several mechanisms by which the ImmA mutants could have increased specific activity, and these could be related to the mechanisms by which RapI and RecA increase the activity of ImmA. The ImmA mutants might have altered conformations that enable them to recognize and/or cleave ImmR more efficiently than the wild type. It is also possible that the mutations allow ImmA to fold more easily or enhance incorporation or retention of metal (presumably zinc) into the protein.

Activation of ICE*Bs1* gene expression by RapI and RecA. ICE*Bs1* gene expression is normally induced by production of active RapI or during the RecA-dependent SOS response (Fig. 1B) (2). The two activation mechanisms are independent of each other in that (i) SOS stimulates induction of ICE*Bs1* in a *rapI* null mutant and (ii) RapI production induces ICE*Bs1* in a *recA* null mutant (2). Both RapI and RecA stimulate ImmA-dependent cleavage of ImmR, and RapI-mediated stimulation appears to be direct, as it occurs in the heterologous host *E. coli* (4). For simplicity, we assume that RecA-stimulated cleavage is also direct, although this has not yet been determined. Attempts to activate ImmA *in vitro* with purified RapI and RecA have not yet been successful.

There are several possible mechanisms by which RapI and RecA could activate ImmA-mediated cleavage of ImmR. Three general possibilities include (i) activation of ImmA, (ii) activation of ImmR, making it a better substrate for ImmA, and (iii) activation by bringing ImmA and ImmR together. It is not clear whether RapI and RecA stimulate ImmA-mediated cleavage of ImmR by the same mechanism. For discussion purposes and for simplicity, we assume that the RapI and RecA work similarly, although this clearly need not be the case.

Isolation of mutations in *immA* that cause significant derepression of ICE*Bs1* gene expression points to ImmA as the target of RapI and RecA. Based on our results, we propose that RapI (and likely RecA) causes induction of ICE*Bs1* gene expression by causing an increase in the specific activity of ImmA and not by causing an increase in its cellular concentration. There are several possible mechanisms by which the specific activity of ImmA might be increased. RapI and RecA

might bind to ImmA to make it favor a conformation that cleaves ImmR faster. Alternatively, they might chaperone ImmA to help it fold properly and to prevent it from forming inactive aggregates. It is also possible that RapI and RecA cause a covalent change in ImmA, although we have not detected any such change and do not favor this possibility.

ImmA and ImmR in other mobile genetic elements. Homologs of ImmA and ImmR are found in many other mobile elements and putative mobile elements (4). The roles of ImmA and ImmR homologs in phage ø105 are similar to those of ImmA and ImmR in regulating ICE*Bs1* (4). The ImmR homolog of phage ø105 represses transcription to maintain lysogeny, and the ImmA homolog is required for induction of lytic growth when the SOS response is induced. Thus, the mode of regulation involving ImmA and ImmR is likely conserved in a variety of other systems. Alignments indicate that many ImmA homologs are shorter than ICE*Bs1* ImmA and are missing the C-terminal 10 to 15 residues (data not shown). In the homologs that are similar in length to ICE*Bs1* ImmA, the C-terminal regions are not conserved. Since the C-terminal residues of ICE*Bs1* ImmA are dispensable and contribute to the instability of ImmA, we suspect that many of the ImmA homologs are likely to be stable and are regulated by controlling the activity and not the amount of the protein. Further characterization of ImmA and the mechanisms by which it is regulated is likely to provide information about the regulation of many agents of horizontal gene transfer.

ACKNOWLEDGMENTS

We thank J. M. Auchtung, C. A. Lee, A. I. Goranov, M. B. Berkmen, and S. E. Cohen for helpful discussions and C. A. Lee, J. Thomas, and K. Menard for comments on the manuscript.

This work was supported in part by an NSF graduate fellowship to B.B. and Public Health Service grant GM50895 from the NIH to A.D.G.

REFERENCES

1. **Auchtung, J. M., C. A. Lee, K. L. Garrison, and A. D. Grossman.** 2007. Identification and characterization of the immunity repressor (ImmR) that controls the mobile genetic element ICE*Bs1* of *Bacillus subtilis*. Mol. Microbiol. **64:**1515–1528.
2. **Auchtung, J. M., C. A. Lee, R. E. Monson, A. P. Lehman, and A. D. Grossman.** 2005. Regulation of a *Bacillus subtilis* mobile genetic element by intercellular signaling and the global DNA damage response. Proc. Natl. Acad. Sci. U. S. A. **102:**12554–12559.
3. **Berkmen, M. B., C. A. Lee, E. K. Loveday, and A. D. Grossman.** 2010. Polar positioning of a conjugation protein from the integrative and conjugative element ICE*Bs1* of *Bacillus subtilis*. J. Bacteriol. **192:**38–45.
4. **Bose, B., J. M. Auchtung, C. A. Lee, and A. D. Grossman.** 2008. A conserved anti-repressor controls horizontal gene transfer by proteolysis. Mol. Microbiol. **70:**570–582.
5. **Burrus, V., J. Marrero, and M. K. Waldor.** 2006. The current ICE age: biology and evolution of SXT-related integrating conjugative elements. Plasmid **55:**173–183.
6. **Burrus, V., G. Pavlovic, B. Decaris, and G. Guedon.** 2002. Conjugative transposons: the tip of the iceberg. Mol. Microbiol. **46:**601–610.
7. **Burrus, V., G. Pavlovic, B. Decaris, and G. Guedon.** 2002. The ICE*St1* element of *Streptococcus thermophilus* belongs to a large family of integrative and conjugative elements that exchange modules and change their specificity of integration. Plasmid **48:**77–97.
8. **Cheo, D. L., K. W. Bayles, and R. E. Yasbin.** 1992. Molecular characterization of regulatory elements controlling expression of the *Bacillus subtilis recA+* gene. Biochimie **74:**755–762.
9. **Churchward, G.** 2002. Conjugative transposons and related mobile elements, p. 177–191. *In* N. L. Craig (ed.), Mobile DNA II. ASM Press, Washington, DC.
10. **Gottesman, S.** 1996. Proteases and their targets in *Escherichia coli*. Annu. Rev. Genet. **30:**465–506.
11. **Harwood, C. R., and S. M. Cutting.** 1990. Molecular biological methods for Bacillus. Wiley, Chichester, England.
12. **Jaacks, K. J., J. Healy, R. Losick, and A. D. Grossman.** 1989. Identification and characterization of genes controlled by the sporulation-regulatory gene *spo0H* in *Bacillus subtilis*. J. Bacteriol. **171:**4121–4129.
13. **Roberts, A. P., and P. Mullany.** 2009. A modular master on the move: the Tn*916* family of mobile genetic elements. Trends Microbiol. **17:**251–258.
14. **Rudner, D. Z., K. S. Breger, and D. C. Rio.** 1998. Molecular genetic analysis of the heterodimeric splicing factor U2AF: the RS domain on either the large or small Drosophila subunit is dispensable in vivo. Genes Dev. **12:**1010–1021.
15. **Salyers, A. A., N. B. Shoemaker, A. M. Stevens, and L. Y. Li.** 1995. Conjugative transposons: an unusual and diverse set of integrated gene transfer elements. Microbiol. Rev. **59:**579–590.
16. **Sambrook, J., and D. W. Russell.** 2001. Molecular cloning: a laboratory manual, 3rd ed. Cold Spring Harbor Laboratory Press, Cold Spring Harbor, NY.
17. **Vasantha, N., and E. Freese.** 1980. Enzyme changes during *Bacillus subtilis* sporulation caused by deprivation of guanine nucleotides. J. Bacteriol. **144:**1119–1125.
18. **Wozniak, R. A., and M. K. Waldor.** 2010. Integrative and conjugative elements: mosaic mobile genetic elements enabling dynamic lateral gene flow. Nat. Rev. Microbiol. **8:**552–563.